e-ISSN: 2146 - 9067

International Journal of Automotive Engineering and Technologies

journal homepage:
https://dergipark.org.tr/en/pub/ijaet

Original Research Article

Effects on ring wear of bioethanol/diesel fuel blends used at long term endurance tests in a DI engine

İlker Temizer[1*], Ayşegül Arı[2]

[1, 2] Sivas Cumhuriyet University, Faculty of Technology, Department of Manufacturing Engineering, Sivas, Türkiye.

ARTICLE INFO

Orcid Numbers
1. 0000-0003-1170-3898
2. 0000-0003-0194-9376

Doi: 10.18245/ijaet.1150240

* Corresponding author
itemizer@cumhuriyet.edu.tr

Received: July 28, 2022
Accepted: Dec 12, 2022

Published: 30 Dec 2022

Published by Editorial Board Members of IJAET

ABSTRACT

In this study, the long-term endurance tests were carried out in a diesel engine that used diesel and 90% diesel + 10% bioethanol fuels. The spray and temperature distributions of two different fuels in the AVL FIRE program also were examined. Tribological and morphological analysis of piston rings were investigated in a single-cylinder direct injection diesel engine using two different fuel types. The test engine used two different fuel types and was operated for approximately 110 hours under part engine load. Renewed rings in each fuelled engine operation were analyzed at Energy Dispersive X-ray Spectroscopy (EDX) and Scanning Electron Microscope (SEM). Results were also compared with the non-worked piston ring. Analysis results saw that abrasive wear was more intense on the first rings at both fuel types. Examining the effect of biofuels on engine wears, short wear lines were found at engine rings using diesel/bioethanol blend fuel compared to diesel fuel. It was being determined that this situation was a result of combustion parameters (such as pressure, and temperature) created with the different fuels used in diesel engines. As a result, that bioethanol has a content of low carbon (C) compared to diesel fuel, making a positive contribution to the reduction of ring wear.

Keywords: Bioethanol, long-term endurance tests, engine tribology, wear, SEM/EDX

1. Introduction

Biomass is a strategic energy source that is renewable, environmentally friendly, and important for the socio-economic development of countries and manufacture of the alternative fuelled engine [1]. Bioethanol, which is one of these sources, has many advantages such as products from local sources, reduction of dependency on crude oil, contribution to exhaust emissions and high octane number etc. It is very important today with its features [2]. Due to these properties, the performance and emission studies of bioethanol fuel used in engines are intensively carried out by many researchers [3-7]. Some investigations emphasized that the low calorific value and cetane number of bioethanol fuel compared to diesel fuel are quite effective on engine performance [8-10]. It has been added at certain proportions to diesel fuel because bioethanol has a low cetane number [11]. Lower C (carbon) rate and the oxygen contained in bioethanol fuel compared to diesel fuel make a significant contribution to the reduction of exhaust emissions [12-14]. Alternative fuel studies in internal combustion engines are mostly based on short-term engine experiments. Long-term endurance tests should be carried out in engines where fuels such as biodiesel, bioethanol, and biogas are used as alternative fuel engines, and determine the degree of suitability of these fuels. Biomass-based fuels used in diesel engines have very important effects on engine tribology and morphology [15]. Eskici et al. carried out long-term endurance tests by using diesel fuel and biodiesel obtained from vegetable oil as fuel in a single-cylinder diesel engine. The use of biodiesel fuel in the engine operated for 150 hours caused more ring wear, on the other hand, metal residues were lower found in the lubricating oil [16]. The short-term use of biofuels as fuel is a promise for users. However, fuels that cause high carbon accumulation could cause deterioration of the lubricating oil and increase wear in long-term applications [17]. A study was conducted by Gulzar et al to determine the effects of biodiesel blends (20% palm biodiesel, 20% jatropha biodiesel and diesel fuel) on lubricating oil and energy losses. The oil samples were collected at regular intervals during the 200-hour test, and then the rheological, tribological and chemical properties of the samples were investigated. The results showed that B20 blended fuels caused lower viscosity and higher acidity in engine oil compared to diesel fuel. In chemical analysis, an increase in fuel residue, abrasiveness and oxidation was observed in engine oil samples in B20 fuel engine tests [18]. Kurre et al. [19] say that fuel dilution and oxidation are the main causes of engine oil contamination, deterioration, and wear of engine parts. In a study conducted by Agarwal et al., long-term durability tests were carried out with diesel oil and linseed oil methyl ester used as fuel in the engine. ICP element (Fe, Cr, Mg, Cu, Co, Zn, Pb) analysis of the sample taken from the lubricating oil was performed. According to the experimental results, lower wear elements in the biodiesel fuel engine were observed [20]. In another study were used biomass fuel and diesel fuel at an engine that was operated for approximately 800 hours. Lubricating oil samples were taken after the oil change (every 100-hours). Physical and chemical conditions, wear residues and contaminants in the oil samples were determined. The test results showed that the use of biofuels in the engine reduced the oil's service life and viscosity, on the other hand, it caused an increase in TBN, oxidation and nitration [21]. In a numerical study done by Iliev, ıt was modelled different ratios of bioethanol at the AVL Boost program. The results obtained at engine speed 1100-6500 rpm showed that more increased bioethanol ratio at blend decreased the engine power, CO and HC while increasing specific fuel consumption [22]. Praptijanto et al. investigated experimental and numerical. effects on a two-cylinder diesel engine of bioethanol (2.5%, 5%, 7.5% and 10% by volume) added to diesel fuel in a certain amount. As a result of this study, bioethanol use in the engine caused a decrease in CO, soot and NO emissions [23]. Today, it is possible to analyze internal combustion engines numerically with the help of many package programs [24-29,31]. Asadi et al. carried out added biodiesel and bioethanol at the rates of 10% (B10, E10) and 20% (B20, E20) to diesel fuel in the ESE Diesel part of the AVL FIRE program. As a result, it was determined that the ıt decreased NO emission was due to the high bioethanol ratio in the blend [30].

Hoang and Pham observed the effects of lubricating oil in a diesel engine that used diesel fuel and jatropha oil biofuel, for 300 hours. It has been determined that the metal residuals in the lubricating oil of the engine using biofuel are higher compared to diesel fuel [33]. Residual elements in the lubricating oil could be determined by using many methods such as Atomic Absorption Spectrometers (AAS), Rotary Disk Electrode Atomic Emission Spectrometers (RDE/AES), Inductively Coupled Plasma of Optical Emission/Atomic mission Spectrometers (ICP-OES/AES/MS) and X-ray Fluorescence (XRF) Spectrometers [34]. Soukayna et al. investigated the variation of metal elements in the lubricating oil subject to vehicle distance using the ICP/OES method. It was emphasized that the rate increase of metals in the lubricating oil was high up to certain distances, and then decreased [39].

In the literature, there are many studies on the use of bioethanol fuels in engines. However, it is seen that most studies on engine performance and exhaust emissions are based on short-term tests. Also, it is seen that alternative fuels used in engines have different effects on engine parts and lubrication systems. To examine the effects of bioethanol blends on a diesel engine, it is necessary long-term tests. Therefore, the effects of bioethanol added to diesel fuel at a certain rate were investigated at long-term engine tests. Thus, a new perspective has been brought to the literature by determining the long-term usability of biomass-based fuels in engines. The effects of combustion parameters (spray distribution, temperature, etc.) are determined by numerical results in the engine in which different fuels are used, and the effects of tribological engine parts are associated.

2. Materials and Methods

In the experiments, 100% diesel (D100) and 90% diesel+10% bioethanol (B10) fuels were used under part load and at 2000 rpm of engine speed, for approximately 110 hours. Detailed technical specifications of the test engine are given in Table 1. Firstly, it was operated D100 fuelled engine, for 110 hours. Then, it was taken first oil sample at end of this progress. This process was repeated for B10 fuel. For both fuel types, at the end of 110 hours of operation, the lubricating oil and the engine's rings (first, second and third rings) were renewed. The tribological analyzes of piston rings were made at the end of testing. The changes on piston rings were investigated using Energy Dispersive X-ray Spectroscopy (EDX) and Scanning Electron Microscope (SEM). Fig.1 shows the experimental setup.

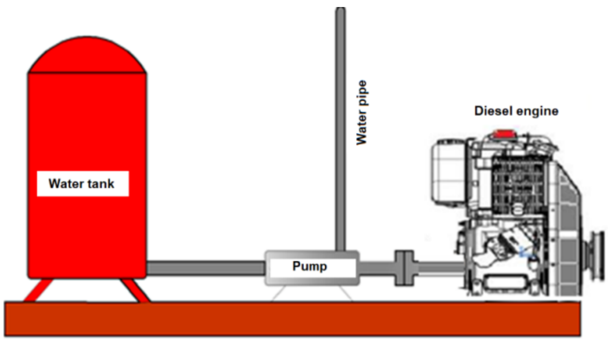

Fig.1 Experimental setup

Table 1. Test engine specifications

Specifications	Descriptions
Engine Type	4- stroke, direct injection diesel engine
Cylinder number	1
Cylinder volume	510 cm^3
Bore x Stroke	85 x 90 (mm x mm)
Compression ratio	17.5:1
Maximum power	8.8 (kW) @3000 (rpm)
Maximum torque	32.8 (Nm) @2000 (rpm)

In the numerical study, ıt was created the combustion chamber model of a single-cylinder, direct injection, Antor 3 LD 510 diesel. In all numerical studies, the spray angle was determined as 126°. Fig.1 show the combustion chamber geometry mesh of a single-cylinder diesel engine. The calculations were carried out at approximately 100000 cells for combustion chambers. In this study, ıt was created the combustion chamber model of a single-cylinder, direct injection, Antor 3 LD 510 diesel. The mesh of the combustion chamber at the top dead centre (TDC) are shown in Fig. 2. In this study, the technical features of the engine were defined in the ESE DIESEL section of the AVL FIRE program and it was modelled. The combustion chamber geometry was based on the full measure of a single-cylinder diesel engine. Initial and boundary conditions for numerical study are given in Table 2.

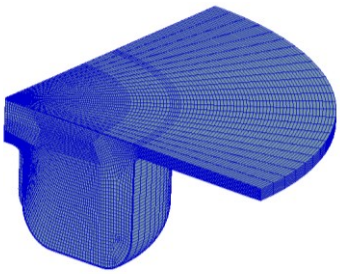

Fig.2. View of the modelled combustion chamber

Table 2. Determined initial and boundary conditions

Specifications	Descriptions
Engine speed	2000 (rpm)
Air inlet temperature	293.15 (K)
pressure	1 (bar)
Fuel injection temperature	330.15 (K)
Cylinder head temperature	575.15 (K)
Cylinder wall temperature	475.15 (K)
Spraying range	305°-329° (CA)
Turbulence model	k-zeta-f model
Spray model	WAVE model
Wall interaction model	Walljet10
Combustion model	Extended coherent flame model – three-zone (ECFM-3Z)

3. Result and Discussion

The spray droplet/crank angle/temperature variations for two different fuel types at an engine speed of 2000 rpm were shown in Fig.3. Depending on the progress of the liquid fuel jet in the combustion chamber and the development of combustion, local temperatures concentrated in the combustion chamber wall regions.

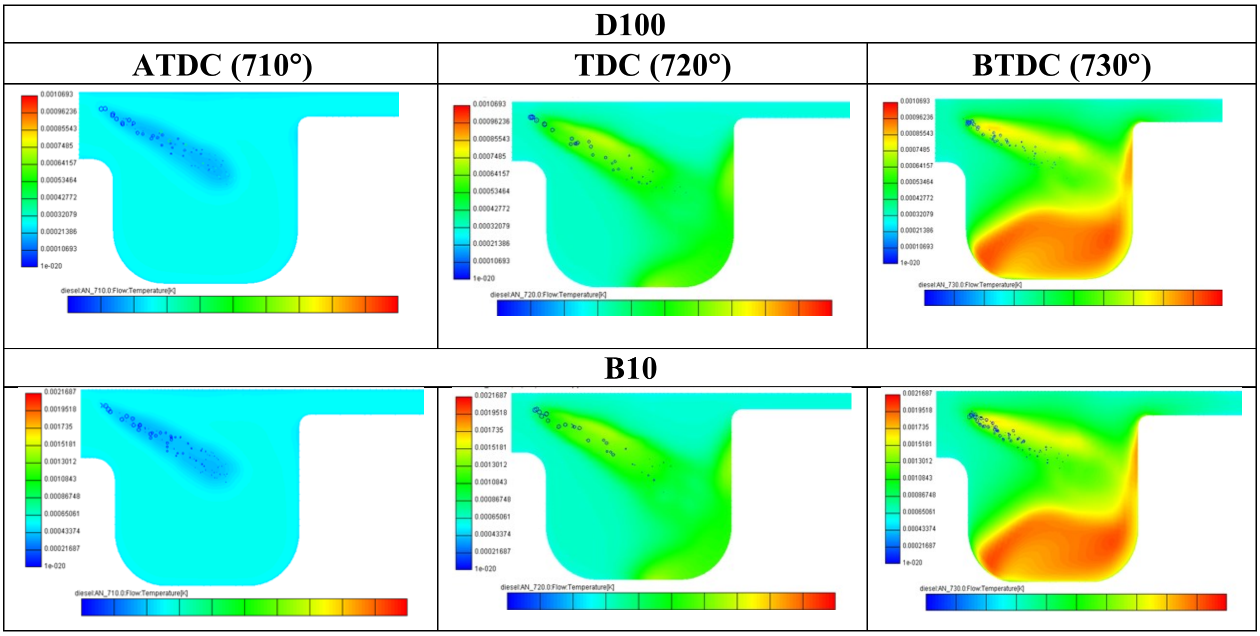

Fig.3. The spray droplet/crank angle/temperature variations for D100 and B10 fuel types

Examining spray/temperature distributions, it was observed that the highest temperature occurred at D100 fuelled operation. This was evaluated as a result of the higher calorific value of D100 fuel, compared to the bioethanol blend [3]. Also, the high heat of evaporation of bioethanol compared to diesel slightly decreased the combustion chamber temperatures. Examined the spray droplet/temperature distributions, it could be said that higher temperatures occurred in the liquid/steam penetration area, for D100 operation at the 730° CA.

The effects of different fuel blends on combustion were investigated in the AVL-FIRE program at 2000 engine speed. In the study, D100 and B10 fuels were selected from the AVL library. The variation of in-cylinder pressures/crank angle (a) and heat release rate/ crank angle (b) at engines that used different fuels are given in Fig.4. It was observed that the maximum in-cylinder pressures for all test fuels were obtained after the 725° CA. Many parameters affect the in-cylinder pressure distribution. Some of these can be listed as fuel density, cetane number, evaporation ability, ignition temperature and calorific value. Examining the in-cylinder pressure distributions, it was seen that the maximum pressures are lower in bioethanol blended fuel compared to D100 fuel. Ethanol has a lower cetane number than diesel fuel [32]. Especially low cetane number causes diesel knock in engines as well as worsening combustion. Due to this feature of ethanol, there are many studies where it is added to diesel fuel at low rates such as 10%, 20% and 30% [40]. When the heat release rates are examined in Fig. 3, it is seen that they are parallel with the in-cylinder pressure distributions. It can be said that the high calorific value of D100 fuel compared to the B10 blend is effective, especially in the maximum pressure and heat releases in the cylinder. It could be said that this situation causes to decrease in maximum cylinder temperatures at the bioethanol blend.

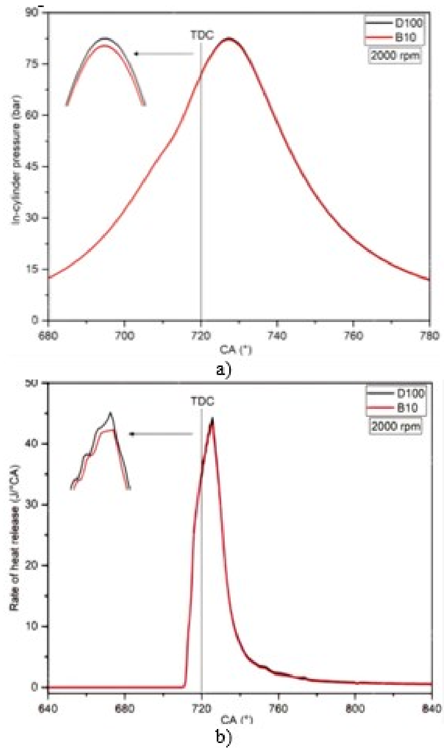

a) b)

Fig.4. The variation of in-cylinder pressures/crank angle (a) and rate of heat release / crank angle (b)

In the tribological analysis of piston rings, it is very important to determine the pressure and temperature changes in the combustion chamber. Increasing pressure and temperature in the cylinder causes an increase in thermal stresses and wear of engine parts. Firstly, SEM/EDX analyses of the first rings of the D100, B10 fuelled engine and non-operation were carried out. Fig. 5 shows SEM/EDX images of the non-operated piston ring at different magnifications. As is known, first rings are exposed to higher temperatures and pressures compared to other rings (compression and oil rings) [28]. This means that first piston rings cause more wear than other rings. Therefore, many manufacturers resort to the coating method, especially on the first ring surface [16]. In EDX analyses, it was seen that the first ring surface was coated with chromium (Cr). In these analyzes, it was observed that surface roughness was given at certain angles (indicated by yellow arrows) to ensure the adhesion of the lubricating oil on the surface. Fig. 6 shows the EDX analysis of the surface at the non-operation first ring.

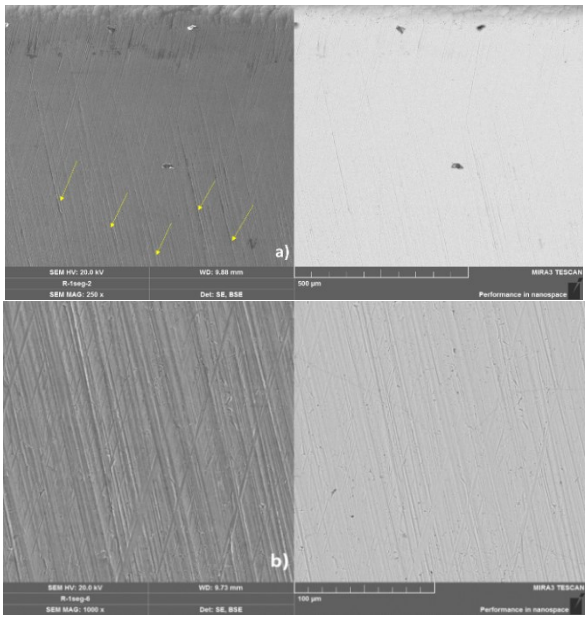

Fig.5. SEM/EDX images of the non-operation first ring, at 250x magnification (a) and at 1000x magnification (b)

Fig.7 shows SEM/EDX images of the first ring at D100 fuelled operation. Compared to the non-operation ring surface, the surface tribology of the first ring at D100 operation appears to have changed considerably. Surface roughness that was seen at the non-operation ring surface completely disappeared ending the D100 fuelled operation.

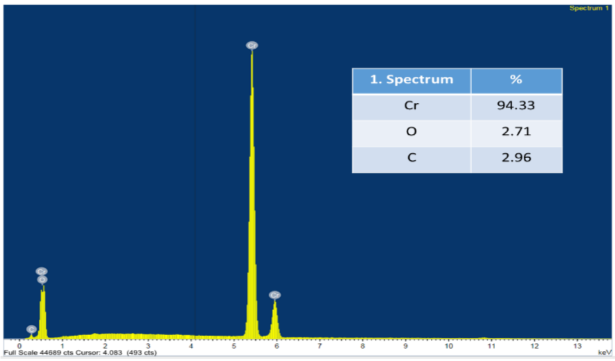

Fig.6. Elemental distribution on the surface of the non-operation first ring

In addition, examining morphologically first ring surface and saw that it created than Cr element. In D100 fuelled operation, it was seen as fatigue wear as well abrasion wear (blue arrows at D100 operation, under 1000x magnification). Linear wear marks mostly occurred on the surface. When Fig.7 (b) is examined, we could say that micro-sources occur in the regions indicated by the red arrows. Fig.9 shows SEM/EDX images of the first ring at the engine-operated B10 fuelled. Comments were made by looking at the incidence and length of the wear lines in the SEM/EDX images. Angular axis lines and surface roughness that was created in the production phase completely disappeared in the B10 operation, as in the D100 fuelled operation. In study B10, it was seen that the element distributions on the first piston ring little changed much compared to the non-operation first ring. While longer wear lines spread over the entire surface of the first ring in the D100 fuel operation, more local and limited wear lines occurred in the B10 operation. In addition, local fretting wear (white arrow at 1000x magnification) was detected at the first ring in the B10 operation. This could be the result of micro-particulate matter boiling into the cylinder wall. In engines, the first rings are exposed to high temperatures and pressure. Therefore, the lubricating film thickness decreases or disappears completely in these regions, depending on the decreasing viscosity of the oil. This results in an increased degree of wear on the working parts. Compared to diesel, the low heating value of ethanol causes a decrease in the indicated pressure and temperature in engines [3]. The decreasing pressure and temperatures in the combustion chamber affected the wear levels of the first rings. Fig.8 and Fig.9 show the EDX analysis of the first surface at D100 and B10 fuelled operation, respectively.

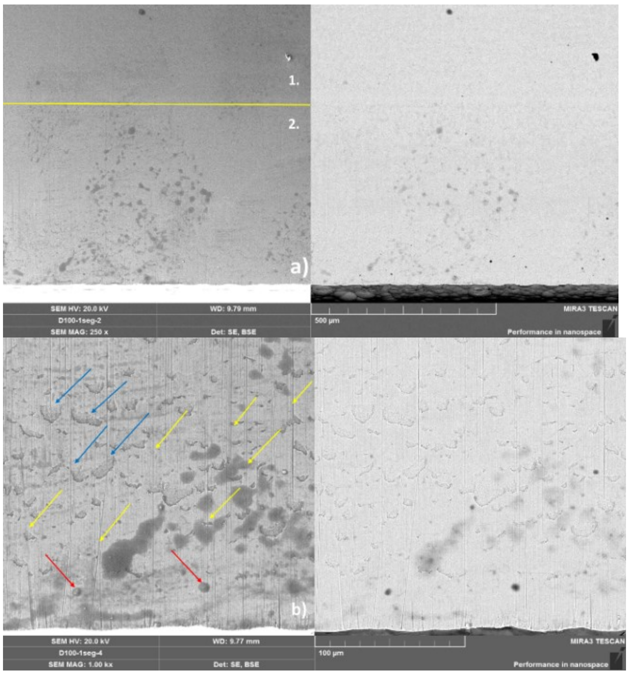

Fig.7. SEM/EDX images of first ring for D100 fuelled operation, at 250x magnification (a) and at 1000x magnification (b)

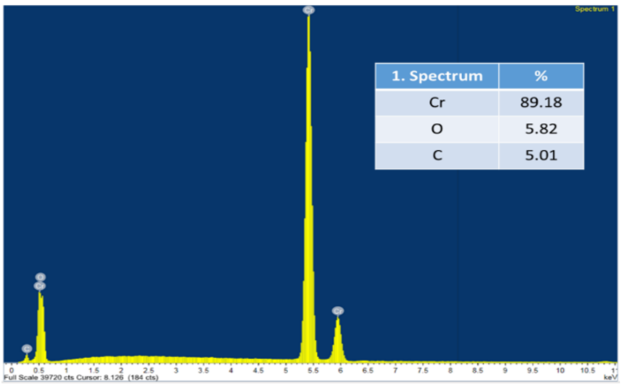

Fig.8. Elemental distribution on the surface of first ring at D100 fuelled operation

Fig.11 shows SEM/EDX image for the non-operated second ring. In both fuel studies, it could be said that the second ring surfaces were less worn compared to the first rings. EDX analysis showed that the surface of the second ring was graphite cast iron. SEM/EDX images showed that the surface was rough to keep lubricating oil on the surface. Fig.12 shows the EDX analysis results reflecting the surface morphology of the non-operation second ring.

Fig.13 shows SEM/EDX images of the second ring at D100 fuelled operation. Examined the second piston ring tribologically at D100 fuelled operation, it was observed that two different areas formed.

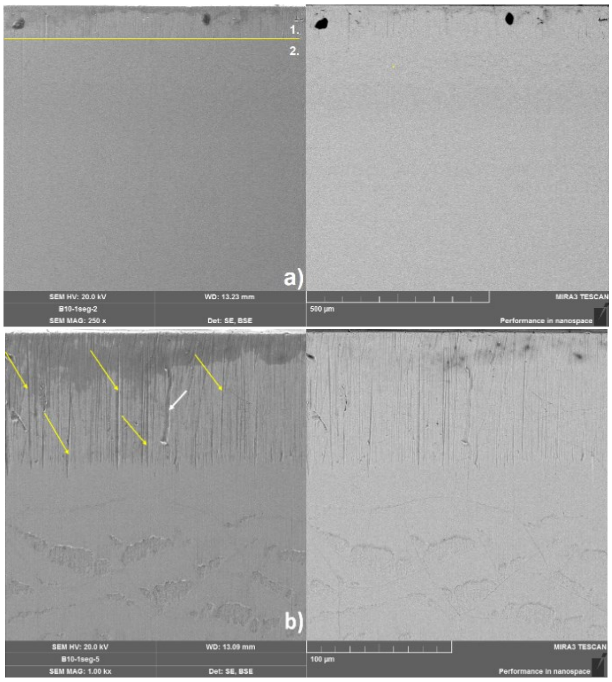

Fig.9. SEM/EDX images of first ring for B10 fuelled operation, at 250x magnification (a) and at 1000x magnification (b)

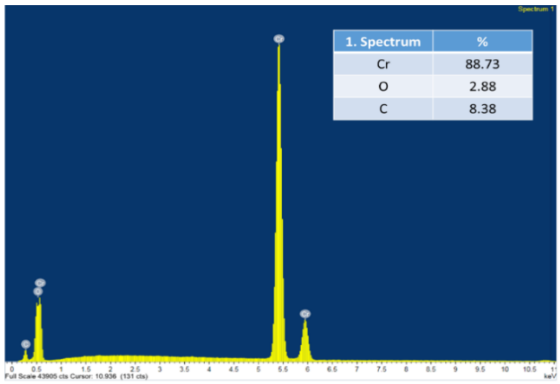

Fig.10. Elemental distribution on the surface of first ring at B10 fuelled operation

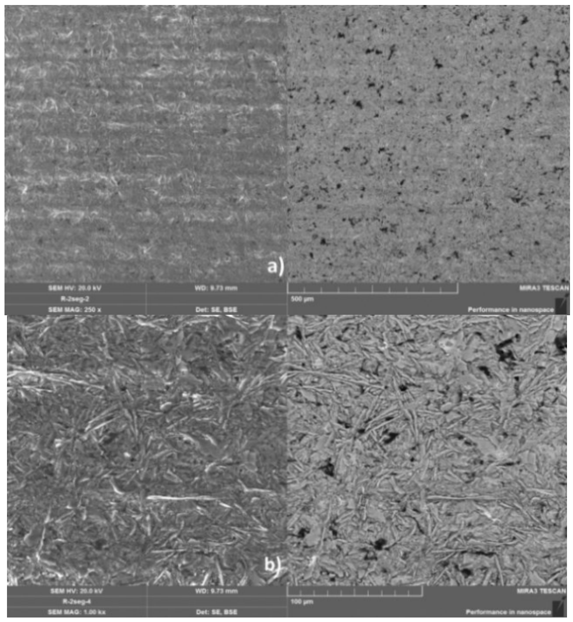

Fig.11. SEM/EDX images of non-operation second ring, at 250x magnification (a) and 1000x magnification (b)

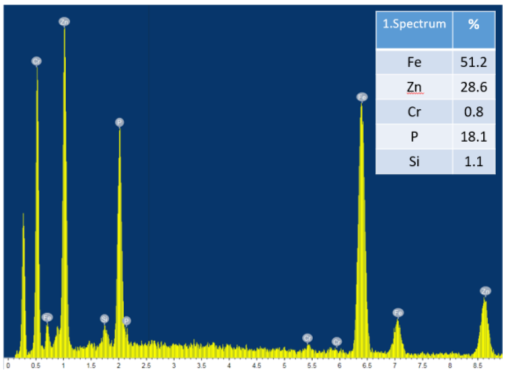

Fig.12. Elemental distribution on the surface of non-operation second ring

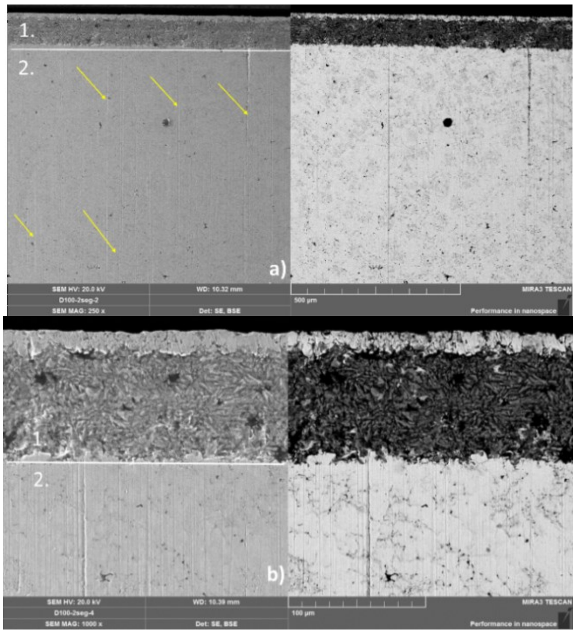

Fig.13. SEM/EDX images of second ring for D100 fuelled operation, at 250x magnification (a) and at 1000x magnification (b)

2nd region (bottom of the yellow line) represents the part of the ring close to the combustion chamber, while 1st region (top of the yellow line) represents the bottom part of the ring. While the porous structure that was seen in the non-operation ring structure was denser in the 1st region, wearing lines were denser in the 2nd region. In the entire 2nd region, it was determined abrasive wear lines which be along the piston line. Examined the element distribution ratios of the surface, while Fe element was determined at the rate of 77.41% by weight in the 1st region, this rate was 85.91% in the 2nd region. Fig.14 shows the EDX analysis of the second ring surface at D100 fuelled operation. C, O, Zn, Mn and P elements at the 1st region of the second ring surface were determined. This result could be considered an indicator of the presence of lubricating oil in this region. Fig.15 shows SEM/EDX images of the second ring at B10 fuelled operation. As in the D100 operation, it could be said that the ring surface formed than two-zone structure at B10 fuelled operation. Also, the presence of a porous structure seen in the second ring is remarkable, as in the non-working ring structure. This issue could be an indication of less worn in B10 operation, compared to the D100. In addition, the abrasive wear liner on the ring was less at the B10 operation. Examined the element distribution ratios of the surface, while Fe element was determined at the rate of 70.73% by weight in the 1st region, this rate was 83.46% in the 2nd region. Fig.16 shows the EDX analysis of the second ring surface at B10 fuelled operation. According to these results, it could be said that the piston ring at the engine used B10 wear more slightly wear compared to the D100 operation.

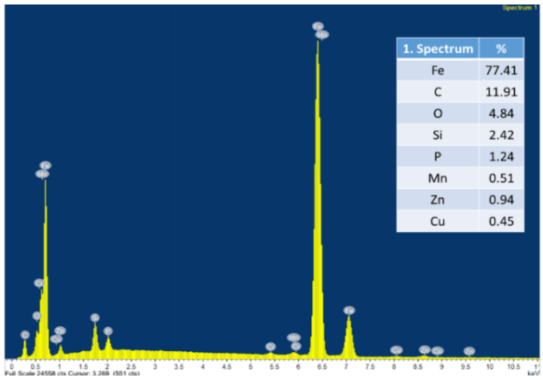

Fig.14. Elemental distribution on the surface of second ring at D100 fuelled operation

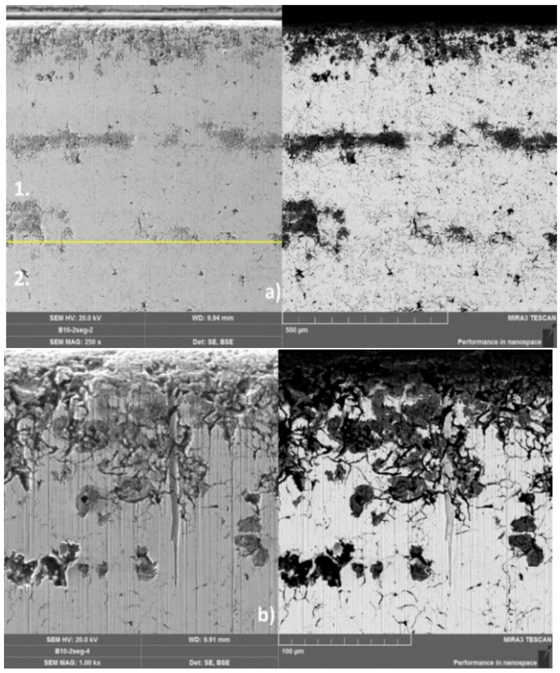

Fig.15. SEM/EDX images of second ring for B10 fuelled operation, at 250x magnification (a) and at 1000x magnification (b)

It was observed that the ratios of elements such as Zn, and P, which were found in high ratios on the non-operating second ring, were considerably reduced at EDX analysis for two fuel types. On the other hand, while Carbon (C) was not found on the non-operating ring surface, it was found at 11.91% on the D100 operating ring surface and 15.93% for the B10. This result could be due to fuel or lubricating oil.

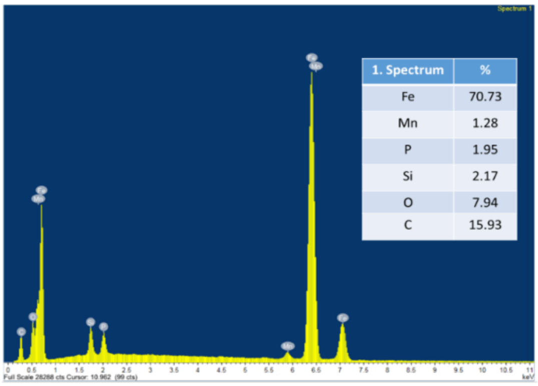

Fig.16. Elemental distribution on the surface of second ring at B10 fuelled operation

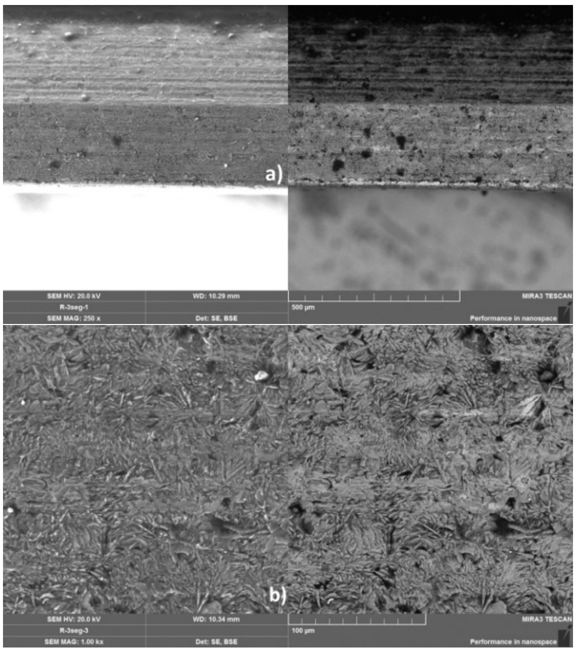

Fig.17. SEM/EDX images of the non-operation third ring, at 250x magnification (a) and at 1000x magnification (b)

Fig.17 shows SEM/EDX images for the non-operated third ring. As a result of 110 hours of operating for all testing fuels, it could be said that the porous surface structure disappeared and the brighter surfaces formed. As well the pressure and temperature distributions formed in the engines as the chemical contents of testing fuels could be effective on wear. The combustion of fuels that have low carbon contents reduces the soot formation in the combustion chamber. Soot formed from the combustion chamber blend to the lubricating oil and its occurrence increases in wear degrees. For this reason, fuels such as bioethanol that included low carbon (C) compared to diesel fuel, make a positive contribution to the reduction of ring wear. Since pressure and temperature formed in the combustion chamber have a lower effect on third rings compared to other piston rings, these piston rings wear less. In addition, third rings were subject to less wear due to their lubricating properties compared to other rings.

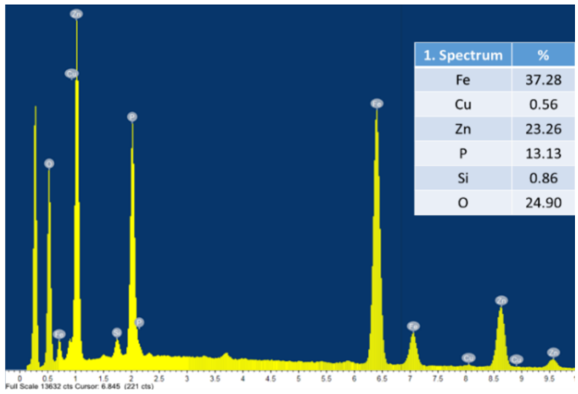

Fig.18. Elemental distribution on the surface of non-operation third ring

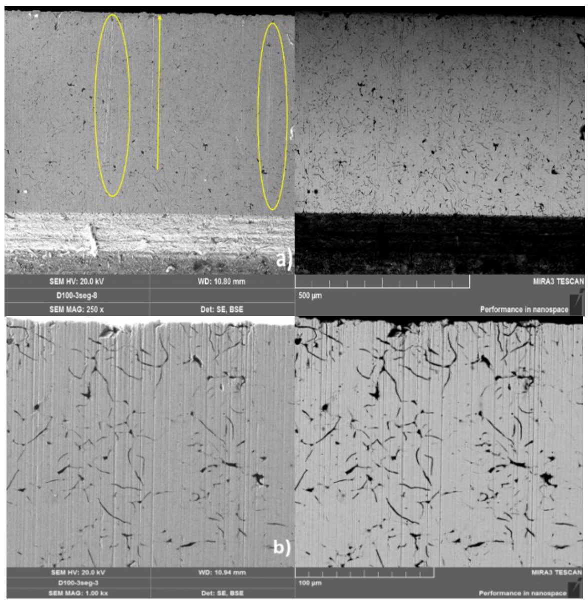

Fig.19. SEM/EDX images of third ring for D100 fuelled operation, at 250x magnification (a) and at 1000x magnification (b)

Fig.19 shows SEM/EDX images of the third ring at D100 fuelled operation. As in second rings, the surface roughness decreased and abrasive wear lines formed along the movement direction of the piston. In D100 fuelled operation, the fretting wear was observed locally (Fig.19, in yellow circles). However, it was seen that the lubricating oil film thickness between the third ring and the cylinder wall was higher than the other rings, which limited the degree of wear. Fig.18, Fig.20 and Fig.22 show the EDX analysis of the third ring surface at non-operating, D100 and B10 fuelled operation, respectively. B10 fuel used in the engine compared to D100 fuel caused the formation of lower wear marks on third ring surfaces. Fig.21 shows SEM/EDX images of the third ring at B10 fuelled operation.

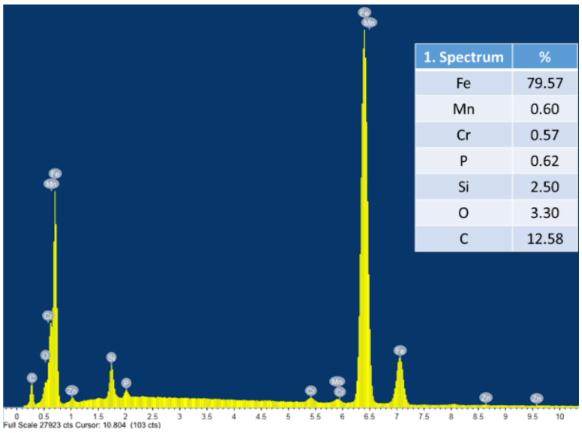

Fig.20. Elemental distribution on the surface of third ring at D100 fuelled operation

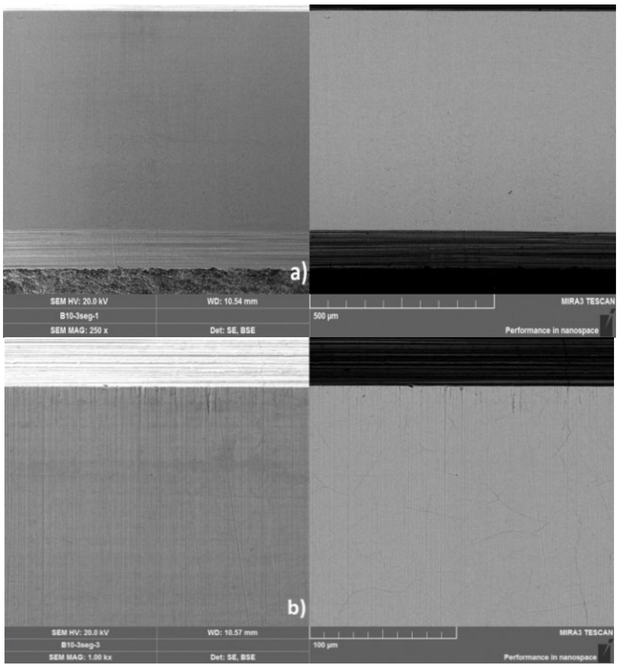

Fig.21. SEM/EDX images of second ring for B10 fuelled operation, at 250x magnification (a) and at 1000x magnification (b)

4. Conclusion

The engine was operated for 110 hours with D100 and B10 fuels. In the study, the combustion analysis and the wear tribology on piston rings were examined together. It is possible to list the results as follows;

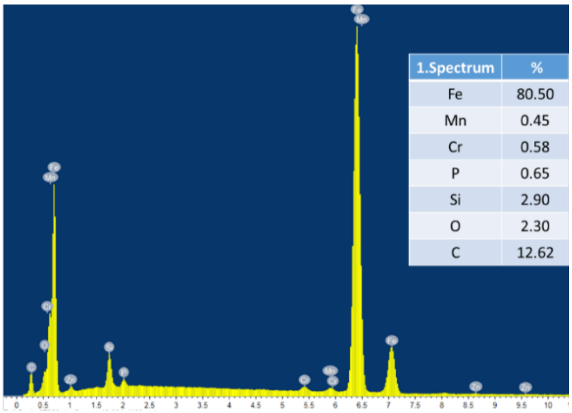

Fig.22. Elemental distribution on the surface of third ring at B10 fuelled operation

- Compared to D100, in B10 operation was seen that combustion end temperatures decreased by approximately 9% due to the low calorific value of the bioethanol fuel and its high heat of vaporization.
- In bioethanol blended operation, pressure and temperatures decreased at the combustion chamber affecting the wear of piston rings. Compared to the D100, fewer wear levels were observed on the first, second and third rings of the engine using B10 fuel.
- For both fuel engine operations, on the ring surfaces occurred mostly abrasive wear lines. However, fatigue and scraping wear debris was observed in some regions of the rings at D100 fuelled operation.
- For all test fuels, the third ring had less surface wear than the other rings, but scraping wear debris was found on the third ring surface in the D100 operation.
- While longer linear wear traces were observed on the rings of the engine using D100 fuel, shorter linear wear traces were detected at the B10 fuelled engine.
- Examined SEM images, it could be said that all rings at the engine used B10 occured more superficially worn compared to D100.

Nomenclature

D100 : %100 diesel fuel
B10 :90% diesel fuel+10% bioethanol (in vol.)
ECFM : Extended coherent flame model
TDC : Top Dead Center
ATDC : After Top Dead Center
BTDC : Before Top Dead Center
EDX : Energy Dispersive X-Ray
SEM : Scanning Electron Microscope
CA : Crank angle

Acknowledgment

This study was supported by TEKNO.030 project number of Cumhuriyet University Scientific Research Projects Unit (CÜBAP).

CRediT authorship contribution statement

No conflict of interest among the authors.

Declaration of Competing Interest

İlker Temizer Writing - original draft, Investigation, Supervision, Conceptualization, Methodology.
Ayşegül ARI. Investigation, Writing-review & editing. Software, Testing.

5. References

1. Patel, C. et. al., Comparative compression ignition engine performance, combustion, and emission characteristics, and trace metals in particulates from Waste cooking oil, Jatropha and Karanja oil derived biodiesels, Fuel, 236, 1366-1376, 2019.
2. Adıgüzel, A. O., General Characteristics and Necessary Feedstock Sources for The Production of Bioethanol, BEÜ Fen Bilimleri Dergisi BEU Journal, 204-220, 2013.
3. İ. Sezer, Experımental ınvestıgatıon the effects of ethanol and dıethyl ether addıtıon ınto dıesel fuel on engıne performance and exhaust emıssıons, J. of Thermal Science and Technology, 37, 1, 61-68, 2017.
4. Paul A., Bose P. K., Panua R., Debroy D., Study of performance and emission characteristics of a single cylinder CI engine using diethyl ether and ethanol blends, Journal of the Energy Institute, 88, 1-10, 2015.
5. Tamilvanan A., Balamurugan K., Ashok B., Selvakumar P., Dhamotharan S., Bharathiraja, M., Karthickeyan, V., Effect of diethyl ether and ethanol as an oxygenated additive on Calophyllum inophyllum biodiesel in CI engine, Environmental Science and Pollution Research, 28, 33880-33898, 2020.
6. Turner D., Xu H., Cracknell R. F., Natarajan V., Chen X., Combustion performance of bio-ethanol at various blend ratios in a gasoline direct injection engine, Fuel, 90, 1999–2006, 2011.
7. Chen R., Okazumi R., Nishida K., Effect of Ethanol Ratio on Ignition and Combustion of Ethanol-Gasoline Blend Spray in DISI Engine-Like Condition, SAE International Journal of Fuels and Lubricants, 8, 2, 264-276, 2015.
8. Nagdeote D., Deshmukh M., Experimental Study of Diethyl Ether and Ethanol Additives with Biodiesel-Diesel Blended Fuel Engine, International Journal of Emerging Technology and Advanced Engineering, 2, 3, 2012.
9. Guido, C., Beatrice, C. ve Napolitano, P., Application of bioethanol/RME/diesel blend in a Euro5 automotive diesel engine: Potentiality of closed loop combustion control technology, Applied Energy, 102, 13-23, 2013.
10. https://msdspds.castrol.com/bpglis/FusionPDS.nsf/Files/2A2A5EA25F6E704E80258408003E5D7E/$File/bpxe-bcm5k9.pdf, 28.11.2021.
11. Rakopoulos D. C., Giakoumis E. G., Dimaratos A. M., Characteristics of performance and emissions in high-speed direct injection diesel engine fueled with diethyl ether/diesel fuel blends, Energy, 43, 214-224, 2012.
12. Kwanchareon P., Luengnaruemitchai, A. ve Jai-In, S., Solubility of a diesel biodiesel-ethanol blend, its fuel properties, and its emission characteristics from diesel engine, Fuel, 86 (7-8), 1053-1061, 2007.
13. Roy M. M., Calder, J., Wang, W., Mangad, A. ve Diniz, F. C. M., Cold start idle emissions from a modern Tier-4 turbo-charged diesel engine fueled with diesel biodiesel, diesel-biodiesel-ethanol, and diesel-biodiesel-diethyl ether blends, Applied Energy, 180, 52-65, 2016.
14. Mofijur M., Rasul, M. G., Hyde, J., Azad, A. K., Mamat, R. ve Bhuiya, M. M. K., Role of biofuel and their binary (diesel-biodiesel) and ternary (ethanol biodiesel- diesel) blends on internal combustion engines emission reduction, Renewable & Sustainable Energy Reviews, 53, 265-278, 2016.
15. Malik M.A.I., Usman, M., Hayat, N., Zubair, S.W.H., Bashir, R., and Ahmed, E., Experimental evaluation of methanol gasoline fuel blend on performance, emissions and lubricant oil deterioration in SI engine. Advances in Mechanical Engineering, 1-17, 2021.
16. Temizer İ., Cihan O., Eskici B., Numerical and experimental investigation of the effect of biodiesel/diesel fuel on combustion

characteristics in CI engine, Volume 270, 117523, 2020.

17. Vikram K., A.K. Avinash, Friction, Wear, and Lubrication Studies of Alcohol-Fuelled Engines, Advances in Engine Tribology, 9-29, 2021.

18. Gulzar M., et.al., Effects of biodiesel blends on lubricating oil degradation and piston assembly energy losses, Energy, 111, 713-721, 2016.

19. Kurre SK, Garg R, Pandey S, A review of biofuel generated contamination, engine oil degradation and engine wear. Biofuels, 8(2), 273-280, 2017.

20. Agarwal A. K., Bijwe, J. ve Das, L. M., Wear assessment in a biodiesel fueled compression ignition engine, Journal of Engineering for Gas Turbines and Power, 125, 820-826, 2003.

21. Suthisripok T., Semsamran, P., The impact of biodiesel B100 on a small agricultural diesel engine, Automotive Engineering Department, College of Engineering, Rangsit University, Thailand, 397-409, 2018.

22. Iliev S. A Comparison of Ethanol and Methanol Blending with Gasoline Using a 1-D Engine Model. Procedia Engineering, 100:1013–1022, 2015.

23. Praptijantoa A., Muharama A, NuR A, Putrasari Y., Effect of ethanol percentage for diesel engine performance using virtual engine simulation tool. Energy Procedia, 68:345–354, 2015.

24. Mohan B, Yang W, Yu W, Tay KL, Chou SK., Numerical simulation on spray characteristics of ether fuels, Energy Procedia 205;75:919 – 924, 2015.

25. Soni DK, Gupta R., Numerical analysis of flow dynamics for two piston bowl designs at different spray angles. Journal of Cleaner Production, 149, 723–734, 2017. https://doi.org/https://doi.org/10.1016/j.jclepro.2017.02.142.

26. Soni D.K., Gupta. R., Numerical investigation of emission reduction techniques applied on methanol blended diesel engine. Alexandria Engineering Journal, 55, 1867–1879, 2016. https://doi.org/10.1016/j.aej.2016.02.019.

27. Temizer İ., Cihan Ö., Analysis of different combustion chamber geometries using hydrogen/diesel fuel in a diesel engine. Energy Sources Part A: Recovery, Utilization, and Environmental, 43, 17-34, 2021. https://doi.org/10.1080/15567036.2020.1811808.

28. Temizer İ., The combustion analysıs and wear effect of biodiesel fuel used in a diesel engine. Fuel, 270, 2020. https://doi.org/10.1016/j.fuel.2020.117571.

29. Rajak U, Nashineb P, Verma TN. Numerical study on emission characteristics of a diesel engine fuelled with diesel-spirulina microalgae-ethanol blends at various operating conditions. Fuel, 262, 2020. https://doi.org/10.1016/j.fuel.2019.116519.

30. Asadi A, Kadijani ON, Doranehgard MH, Bozorg MV, Xiong Q, Shadloo MS, Li KB, Numerical study on the application of biodiesel and bioethanol in a multiple injection diesel engine. Renewable Energy, 150, 1019-1029, 2020.

31. Koca F., Zabun M., The effect of outlet location on heat transfer performance in micro pin-fin cooling used for a CPU, European Physical Journal Plus, 136, 11, 2021. https://doi.org/10.1140/epjp/s13360-021-02113-4.

32. Yüksel, T., Temizer, İ., Can, İ., Koca, F., Investigation of the Using Heated Bioethanol as a Dual Fuel in a Gasoline Engine, Fırat University Journal of Engineering Sciences, 31 (1), 67-77, 2019.

33. Hoang A.T., Pham, P.P., A study of emission characteristic, depoits, and lubrication oil degradation of a diesel engine running on preheated vegetable oil and diesel oil, 1556-7036, 2018.

34. Agarwal A.K., Dhar A., Karanja oil utilization in a direct-injection engine by preheating. Part 2: experimental investigations of engine durability and lubricating oil properties. Proc IMechE Part D: J Automobile Eng 224 (1),85–97, 2009.

35. Agarwal A.K., Dhar A., Wear, durability, and lubricating oil performance of a straight vegetable oil (Karanja) blend fueled direct injection compression ignition engine. J Renew Sust Energy 4 (6), 063138, 2012.

36. Dhar A., Agarwal A.K., Experimental investigations of effect of Karanja biodiesel on tribological properties of lubricating oil in a compression ignition engine. Fuel, 130, 112–9, 2014.

37. Singh S.K., Agarwal A.K., Srivastava D.K., Sharma M., Experimental investigations of the effect of exhaust gas recirculation on lubricating oil degradation and wear of a compression ignition engine. ASME J Eng Gas Turbines 128, 921–7, 2006.

38. Gopal K.N., Raj R.T.K, Effect of Pongamia oil methyl ester–diesel blend on lubricating oil degradation of di compression ignition engine, Fuel 165 105–114, 2016.

39. Soukayna Z., Mohammed M., Jamal N., Physicochemical Characterization of the Synthetic Lubricating Oils Degradation under the Effect of Vehicle Engine Operation, Eurasian Journal of Analytical Chemistry 13 (4), 2018.

40. Jayaprabakar J., Anish M., Beemkumar N., Mathew A., George A. A., Effect of diethyl ether blended with neem oil methyl esters in CI engine, International Journal of Ambient Energy, 40, 116-118, 2017.